Cold Regions Science and Technology 81 (2012) 26–35

Contents lists available at SciVerse ScienceDirect

Cold Regions Science and Technology

journal homepage: www.elsevier.com/locate/coldregions

Numerical simulations of a tanker collision with a bergy bit incorporating hydrodynamics, a validated ice model and damage to the vessel

R.E. Gagnon *, J. Wang

Ocean, Coastal and River Engineering, National Research Council of Canada, St. John's, NL, Canada A1B 3T5

ARTICLE INFO

Article history:
Received 8 March 2012
Accepted 16 April 2012

Keywords:
Bergy bit collision
Numerical simulation
Ship damage

ABSTRACT

Numerical simulations of a collision between a loaded tanker and a bergy bit have been conducted using LS-Dyna™ software. The simulations incorporated hydrodynamics, via LS-Dyna's ALE formulation, and a validated crushable foam ice model. The major portion of the vessel was treated as a rigid body and a section of the hull, located on the starboard side of the forward bow where the ice contact occurred, was modeled as typical ship grillage that could deform and sustain damage as a result of the collision. Strategies for dealing with the highly varying mesh densities needed for the simulations are discussed as well as load and pressure distribution on the grillage throughout the course of the collision. Realistic movement of the bergy bit due to the vessel's bow wave prior to contact with the ice was observed and the damage to the grillage resembled published results from actual grillage damage tests in the lab. A load measurement from the lab tests compared reasonably well with a rough estimate from the simulation. The collision eventually ruptured the hull in a ripping fashion resembling documented incidents of vessel impacts with ice masses.

1. Introduction

Marine transportation off the East Coast of Canada is seriously affected by the presence of glacial ice masses. The same can be said for Arctic regions and areas off the west coast of Greenland where there are new hydrocarbon prospects. This is a problem for tanker transport of crude oil from current and future offshore production facilities, and for the transport of supplies to northern communities such as Churchill Manitoba and minerals from Labrador. Of most concern for supply ships and tankers are bergy bits (house-sized glacial ice masses), which are difficult to detect using marine radar in rough sea states and when imbedded in sea ice flows. Should these make contact with a ship's hull, the impact forces will depend on the masses of the vessel and ice, the hydrodynamics of the interaction, the ship structure, the shape of the ice mass and its local crushing properties.

NRC Ocean, Coastal and River Engineering has been studying various aspects of the problem for several years, with the overall objective of creating a validated numerical model of ship/bergy bit collisions. The work has involved extensive physical model testing of a tanker transiting in proximity to bergy bits in NRC's Tow Tank (Gagnon, 2004a), impact experiments in NRC's Ice Tank using real growlers (Gagnon, 2004b) and strength and crushing experiments on iceberg ice and lab-grown ice (e.g. Gagnon, 2004c; Jones et al., 2003). A field study involving bergy bit impacts with an instrumented ship was also conducted (Gagnon et al., 2008). In parallel with the experimental aspects of the project the numerical simulation work has been progressing. The data acquired in the Tow Tank proximity tests, growler impact tests and the field study are invaluable assets for the validation of the numerical model. The computational work has involved simulations of the CCGS Icebreaker Terry Fox colliding with a bergy bit (Gagnon and Derradji-Aouat, 2006), simulations of the growler impact lab tests (Gagnon, 2007) and the development of a numerical ice model that incorporates spalling behavior (Gagnon, 2011).

Recently simulation results were obtained for a loaded tanker colliding with a substantial bergy bit. The model tanker had actual ship grillage on a portion of its bow where the collision occurred that could sustain damage during the collision. This is the first simulation of a vessel colliding with a glacial ice mass that includes the hydrodynamics of the interaction, a validated ice model and damage to the vessel associated with the collision. The purpose of this paper is to show the techniques that were utilized to deal with the various challenging aspects of simulations such as this and to show that reasonable results were obtained for a realistic collision scenario. Using readily available hardware and commercial software it is obvious that these same methods can be applied to a wide variety of ship-ice collision cases.

2. Overview of the planned program of simulations

Below we present the techniques, configuration details and results from numerical simulations for one particular scenario. This is part of

* Corresponding author.
E-mail address: robert.gagnon@nrc.ca (R.E. Gagnon).

0165-232X/$ – see front matter. Crown Copyright © 2012 Published by Elsevier B.V. All rights reserved.
doi:10.1016/j.coldregions.2012.04.006

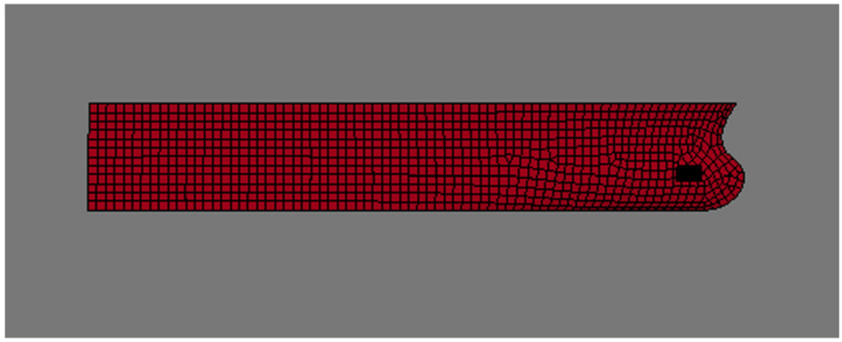

Fig. 1. Side view of the meshed tanker half-ship. The small dark rectangle at the bow is the grillage segment. Only the front half of the vessel is necessary for the simulation.

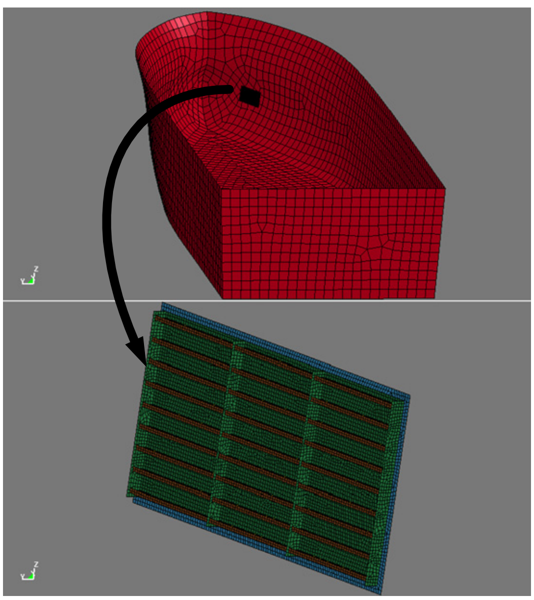

Fig. 2. Perspective view of the meshed tanker half-ship (top) showing the location of the meshed grillage segment (bottom) on the starboard bow. The differing element sizes between the vessel and the grillage segment are evident. The rectangular attachment frame is at the periphery of the grillage segment.

a broad plan for simulation studies that could be used as a tool for ship designers and for those who draft operational strategies, and for the general improvement of codes and rules. In the next few years simulations for a variety of vessel and grillage types will be conducted where the influences of ship speed and impact trajectory, and ice mass size, shape and orientation will be investigated.

Table 1
Ship details.

Dimensions	145 m half length; 48 m beam; 23.9 m depth; 18.9 m draft
Vessel type	Tanker with bulbous bow
Displacement	~ 170,000 ton (full length ship, fully loaded)
Velocity	5.14 m/s (10 knots) after 10 s start-up
Initial ship-ice separation	96 m (from bulbous bow to ice knob)
Element type	*SECTION_SHELL
Typical element dimension	2 m
Material properties	*MAT_RIGID
Number of elements	3432

Table 2
Water box details.

Dimensions	344 m × 144 m × 40 m
Density	1000 kg/m^3
Fluid computational method	ALE (Arbitrary Lagrangian–Eulerian)
Element type	*SECTION_SOLID (brick)
Typical element dimension	2 m
Material properties	*MAT_NULL
Number of elements	247680

What must be conducted in parallel with simulations is a program of validation. To the extent possible, simulation results have to be validated with results from various carefully designed lab and field studies. No single organization that presently exists could undertake all aspects of that work so we anticipate that in the coming years various organizations will, possibly to an even greater extent than in the past, conduct lab and field studies to provide crucial validation data for numerical simulations. For its part, in addition to the activities mentioned above, NRC has worked with collaborators on various field

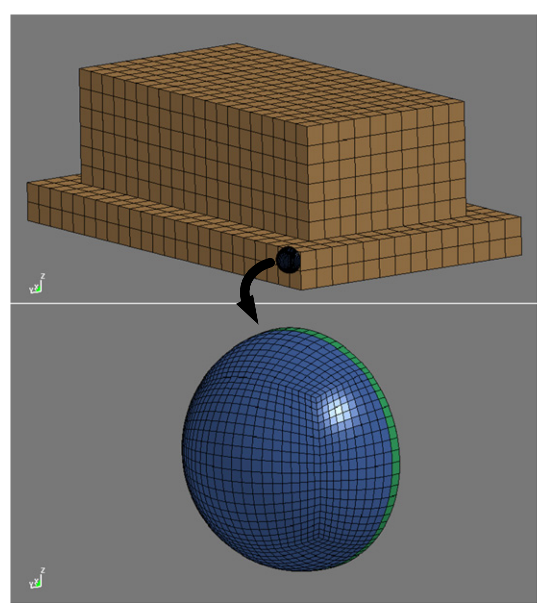

Fig. 3. View of the ice knob (bottom) and its location on the bergy bit ice mass (top). The differing element sizes between the ice knob and ice mass are evident. The bottom layer of elements at the base of the ice knob is treated as a rigid body that is connected to its companion rigid body, i.e. the ice mass. The rest of the elements of the ice knob are deformable with crushable foam properties during the collision.

Table 3
Ice mass details.

Dimensions: lower portion	48 m × 28 m × 4 m
Dimensions: upper portion	40 m × 20 m × 12 m
Density and mass	870 kg/m^3; 13000 ton
Element type	*SECTION_SOLID (brick)
Typical element dimension	2 m
Material properties	*MAT_RIGID
Number of elements	1872

Table 4
Air box details.

Dimensions	344 m × 144 m × 20 m
Density	1.1845 kg/m^3
Fluid computational method	ALE (Arbitrary Lagrangian–Eulerian)
Element type	*SECTION_SOLID (brick)
Typical element dimension	2 m
Material properties	*MAT_NULL
Number of elements	123840

experiments aimed at understanding ice crushing behavior. It also participates in MUN's (Memorial University of Newfoundland) STePS2 (Sustainable Technology for Polar Ships and Structures) Project where large-scale ice crushing and impact experiments, which incorporate real ship grillage, are planned for the near future in MUN's Structures Lab. Additionally, NRC has for some years been preparing and testing components of a novel impact panel in order to conduct another major field study involving an instrumented vessel colliding with bergy bits.

3. Hardware, software and ice model

The simulations were run on a HP Z800 Workstation that has two Intel Xeon Processors X5570 QC, where each has 4 CPU's running at 2.93 GHz. The system has 8 GB of DDR3 RAM. Four CPU's with SMP (single memory processing) were used for the simulation. The software used was LS-Dyna™ version Ls971d Dev, Revision 63221, double precision. It uses LS-Dyna's ALE formulation to handle fluid hydrodynamics and it has a number of contact algorithms and a large suite of material types that can be chosen for the interacting structures. ANSYS Workbench V12.1 with ANSYS DesignModeler™ was used for the modeling and generation of meshes for the study.

A crushable foam model was used for the ice that made contact with the vessel during the simulations. The isotropic foam model crushes one-dimensionally with a Poisson's ratio that is essentially zero, as described by Hallquist (1998). Unloading is elastic to the tension cutoff stress. Subsequent reloading follows the unloading curve. In the implementation it is assumed that Young's modulus is constant and the stress is updated assuming elastic behavior.

$$\sigma_{ij}^{trial} = \sigma_{ij}^{n} + E\dot{\varepsilon}_{ij}^{n+1/2}\Delta t^{n+1/2} \tag{1}$$

where σ_{ij} is the stress tensor, E is the Young's modulus, $\dot{\varepsilon}_{ij}$ is the strain rate tensor and Δt is the time increment. The magnitudes of the

Table 5
Grillage segment details.

Dimensions	6 m length × 3 m height
Plate thickness	10 mm
Frame thickness and height	8 mm × 200 mm
Frame T-top thickness and width	10 mm × 75 mm
Frame spacing	350 mm
Stringer thickness and height	8 mm × 250 mm
Stringer spacing	2 m
Density	7850 kg/m^3
Young's modulus	200 GPa
Plastic tangent modulus	1.0 GPa
Poisson's ratio	0.30
Yield strength	350 MPa
Rupture strength	600 MPa
Element type	*SECTION_SHELL (Hughes-Liu)
Typical element dimension	0.06 m
Material type	*MAT_PIECEWISE_LINEAR_PLASTICITY
Number of elements	12592 (grillage) + 661 (rigid attachment frame)

Table 6
Ice knob details.

Dimensions	1.4 m radius hemisphere
Density	870 kg/m^3
Young's modulus	9.0 GPa
Poisson's ratio	0.003
Element type	*SECTION_SOLID (brick)
Typical element dimension	0.04 m–0.14 m (mean: 0.09 m)
Material properties	*MAT_CRUSHABLE_FOAM
Number of elements	26000 (ice knob) + 2000 (rigid base)

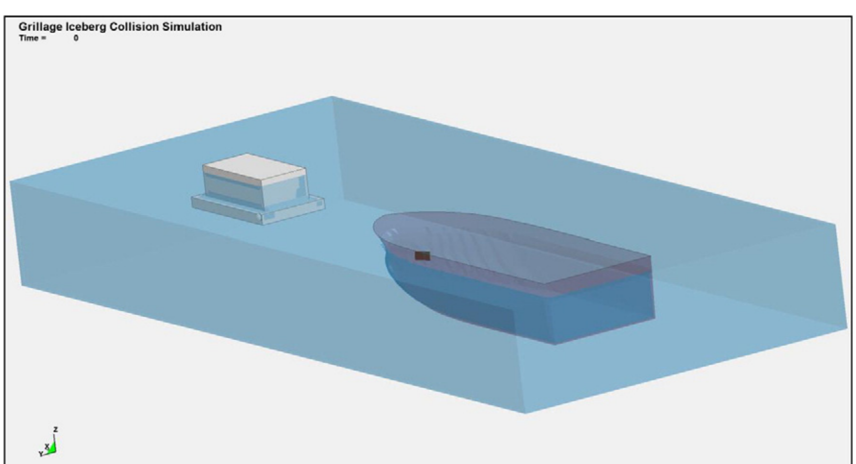

Fig. 4. Full view of simulation components. The bergy bit and tanker half-ship are partially submerged in the water volume. The deformable ship grillage is the small dark rectangle on the starboard bow of the vessel. Not showing is a layer of air above the water that is a required component of the simulation to give the water a free surface. The ice knob, barely visible at this scale, is at the corner of the ice mass nearest to the viewer.

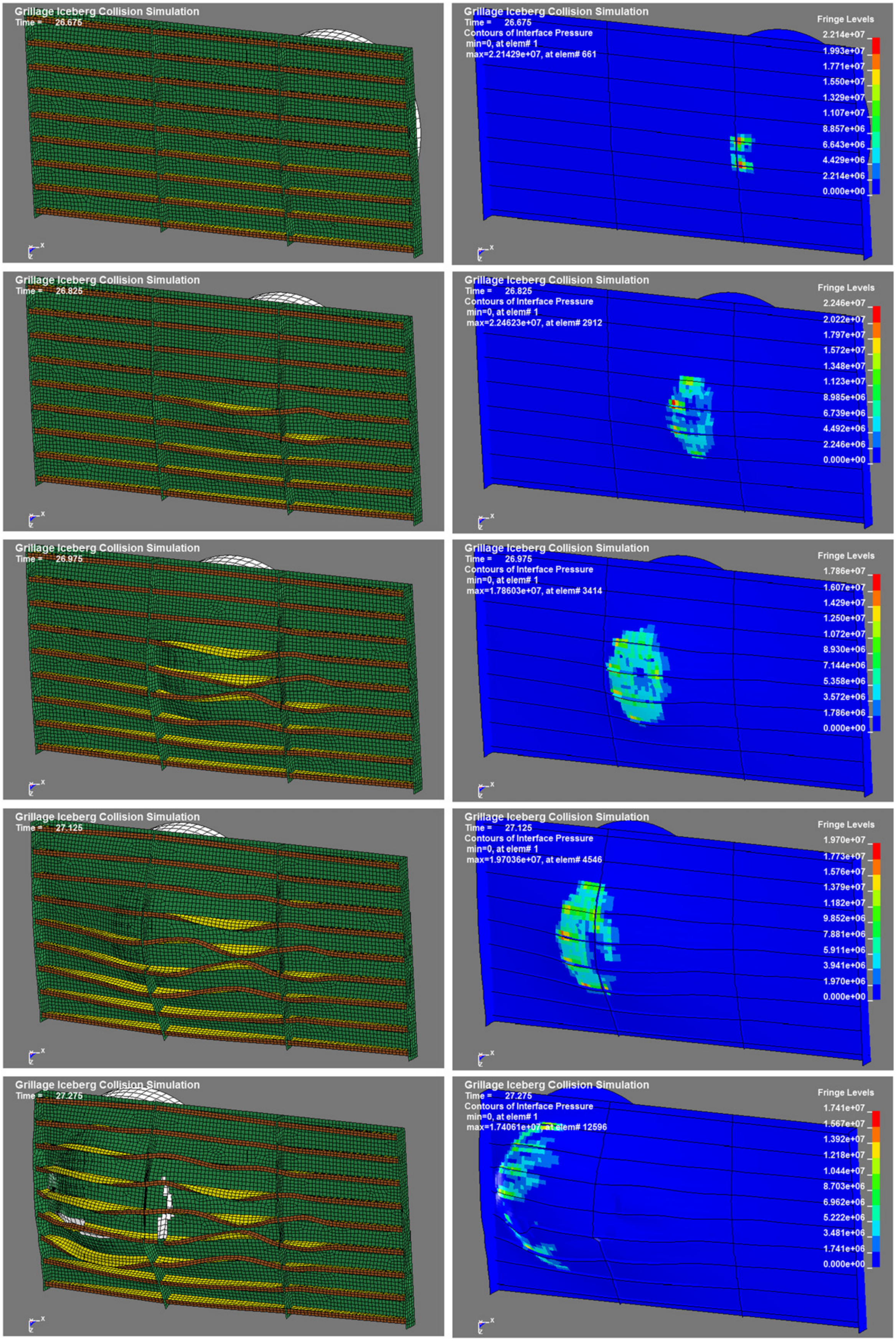

Fig. 5. Simulation image pairs showing grillage damage (left) and interface pressure distribution (right) during the bergy bit impact. The respective image pair times from top to bottom are 26.675 s, 26.825 s, 26.975 s, 27.125 s and 27.275 s. The right hand images have had the frame and stringer components partially removed to make the pressure patterns more visible. The tanker was traveling at 5.14 m/s. The bergy bit mass was 13,000 ton.

principal values are then checked to see if the yield stress is exceeded and if so they are scaled back to the yield surface, σ_y:

$$\text{if } \sigma_y < \left|\sigma_i^{\text{trial}}\right| \text{ then } \sigma_i^{n+1} = \sigma_y \frac{\sigma_i^{\text{trial}}}{\left|\sigma_i^{\text{trial}}\right|} \tag{2}$$

After the principal values are scaled, the stress tensor is transformed back into the global system. The yield surface for the present application has been previously described (Gagnon and Derradji-Aouat, 2006).

Application of a pressure, prescribed by the user, on a block or layer of such foam that is rigidly supported from below causes it to irreversibly compress in the direction of the applied load.

4. Numerical simulation model components and results

The major challenge in the simulation was dealing with the extreme variation of mesh size that is necessary to enable a large vessel to move through water for some distance in order to produce a reasonable bow wave, that requires a coarse mesh, and then having a much finer mesh for the region on the vessel and on the ice where the two objects are in contact during the collision. This is challenging from two perspectives. One is that generally in simulations the objects that are interacting must have compatible mesh sizes. Secondly, there are practical limitations to the smallness of the size of the elements that are used in a simulation since the time step is determined by the size of the smallest element in the mesh. Furthermore if all the elements are small then there is a huge number of them involved in the computations. Either or both of these factors can lead to extremely long run times. So, one has to limit the number of elements that must be of small size and find ways of enabling the fine-mesh components of the ice mass and ship to properly interact while also enabling the much larger components of the ship and ice, that have coarse mesh, to interact with the surrounding water which has roughly the same large element size. This was accomplished using the following methods.

First the vessel (Figs. 1 and 2) was meshed with rigid shell elements of large size (Table 1) that matched the element size of the water (Table 2). The tanker model was a typical loaded oil tanker with dimensions given in Table 1, where only the front half of the ship was needed for the simulation. Similarly the bulk ice mass (Fig. 3) was meshed with rigid brick elements of similar size (Table 3). The tanker was initially located in a body of water with dimensions as in Table 2. Fig. 4 shows the ice mass and vessel in the water volume. There is a layer of air (not visible) above the water (dimensions in Table 4) that is a required component of the simulation to give the water a free surface. Note that we gave the ice mass a brick shape that had a submerged shelf around the bottom periphery. Underwater protrusions are common with floating glacial ice masses.

A segment of ship grillage (Fig. 2), meshed with small shell elements (Table 5), was attached to the vessel at the location where the contact was determined to occur (using the trial and error method described below). To do this, first a rectangular rigid-body attachment frame was meshed with fine mesh elements and connected to the rigid-body ship using the command '*CONSTRAINED_RIGID_BODIES'. Then the deformable grillage segment was secured to the attachment frame by merging the nodes around its periphery that overlapped the inner nodes of the attachment frame. Hence, the grillage segment and the ship bow shell elements partially overlapped one another in space but there was no contact definition between them so they did not interact with each other except where the nodes merged around the periphery. The grillage segment elements also had no contact definition with the water. Hence, the ship was enabled to interact with the water in the area where the grillage was attached so that normal hydrodynamics took place during the ship transit to the impact location and during the collision.

In a similar fashion a relatively small portion of the ice mass in the region where the contact will occur during the collision is shaped as a hemisphere (Fig. 3) and has small mesh elements (Table 6) that match the mesh element size of the ship grillage on the vessel. This hemispherical feature partially consists of a circular base of rigid brick elements that attaches to the main bulk of the large ice mass via the rigid body connection command '*CONSTRAINED_RIGID_BODIES'. The remaining portion of the hemisphere is attached to the base by merging all the nodes at the interface between the two components. We refer to the small hemispherical ice feature as the ice knob.

Note that the specifics of the grillage, as in Table 5, indicate that it is not an ice-strengthened grillage such as would be found on an ice-strengthened ship or FPSO, and is considerably weaker. It is more typical of grillage used on small dry bulk carrier vessels. We chose to use this grillage because damage tests have been performed in the lab on grillage with similar specifications so we can make some comparisons with our results. The methods we employ here, of course, can be used to incorporate any type of grillage onto a vessel in a simulation.

The hydrodynamics of the water during the ship transit and eventual collision with the ice mass was handled by LS-Dyna's ALE method. The ALE method produces realistic looking waves and ice motions due to the vessel's bow wave. Furthermore in previous comparisons of results from simulations with physical model experiments of a tanker transiting in proximity to bergy bits good quantitative agreement was obtained (Gagnon and Derradji-Aouat, 2006). The ship shell elements and water interacted via the LS-Dyna coupling command '*CONSTRAINED_LAGRANGE_IN_SOLID'.

The LS-Dyna command '*INITIAL_VOLUME_FRACTION_GEOMETRY' was used to remove water from the space occupied by the vessel and the ice mass.

Prior to performing the full simulations a short parametric study of element size was conducted to confirm that the element size used in the full simulations was adequately small. Three element sizes were tested, 3 m, 2 m and 1 m. The test scenario was one where the tanker transited in close proximity to the bergy bit and the sway of the bergy bit due to the bow wave of the tanker was used as the measurement index. The simulation results showed that convergence occurred for the 2 m and 1 m element size. Hence, a 2 m element size was deemed adequate for the large-mesh components of the simulation. A similar strategy was used by Gagnon and Derradji-Aouat (2006) to find a suitable element size in preparation for numerical simulations of bergy bit collisions with the CCGS Icebreaker Terry Fox.

To continue, a series of simulations were run where the vessel was given a certain speed (5.14 m/s) to determine a suitable initial placement and orientation for the ice mass in the water in order to get a 'hit' at a suitable location on the bow of the vessel below the waterline. For these simulations all solid components, that is the vessel, the grillage and attachment frame, the ice mass and the ice knob and attachment disk, had rigid body designations so the simulations could run quickly. That is, during the relatively long real time portion of the simulation where the ship is transiting over a distance of ~96 m, in order to generate a realistic bow wave, the simulation runs with a reasonably long time step. That time step is determined by the ship and water mesh element size and not the small elements of the grillage and the ice knob because the latter were given rigid body properties for this stage of the simulation and they have no contact definition with the water. This procedure took about 5 simulations to perform, where each took 12 hr to run, corresponding to 26.3 s of simulation time, and where the time step was 4.7×10^{-4} s. Once the initial placement and orientation for the ice mass in the water was determined then the ice knob was oriented appropriately on the corner of the ice mass so that the base of the knob was parallel with the surface of the grillage segment at the time when contact would occur.

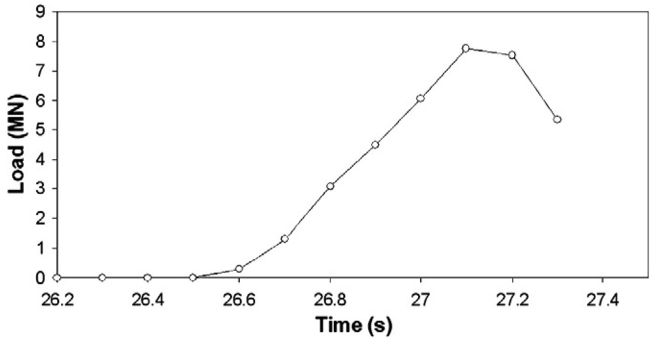

Fig. 6. Load versus time for the collision interaction between the grillage segment of the tanker and the ice knob of the ice mass. Note that since the grillage is deforming during the interaction the force is the resultant force of all the single element forces where contact occurs. While the single element forces may be considered as normal to the respective elements, since the friction force is negligible, the resultant force is not normal to the original grillage surface except perhaps in the very early stages of contact where little deformation has occurred. That is, the elements in the deformed contact area are no longer parallel to the original grillage surface. When significant deformation and gouging has gotten under way the resultant force vector leans back from the original normal, away from the direction of motion, because gouging requires a component of force in the forward direction in addition to a component that is normal to the original grillage surface.

So far what we have described will get the simulation to the point where the vessel is at a close approach to the ice mass and the mass has begun to respond significantly to the hydrodynamics associated with the ship's bow wave. This takes 12 hr of run time. Essentially the grillage segment and the ice knob have not been participating in the simulation to this point because they have been treated as rigid bodies that have no interaction with the water or the vessel, so their small element size has not caused excessively long run times for the simulation. But just before the actual collision occurs it is necessary for these components to be activated, that is, their properties need to be changed to realistic ones rather than simple rigid body ones. In LS-Dyna this cannot be done 'on the fly' during a simulation. A restart is required using the command 'small restart input deck'. That means stopping the simulation just before contact occurs (at time = 26.3 s) and saving all the simulation data up to that point. Then, when the simulation is restarted at the same point in time where it left off the LS-Dyna command '*RIGID_DEFORMABLE_R2D' is used to activate the ice knob and grillage components as deformable parts. Now, however, the time step is much smaller (2.4×10^{-6} s) due to the smaller elements of the ice knob and grillage so the simulation runs much more slowly, i.e. it takes ~73 hr for the remaining simulation time segment from 26.3 s to 27.15 s. Hence the total run time for a simulation is ~85 hr. Note that the simulation ran on only 4 CPU's. Workstations are presently available with ten times this number of CPU's, and Beowulf computer clusters have

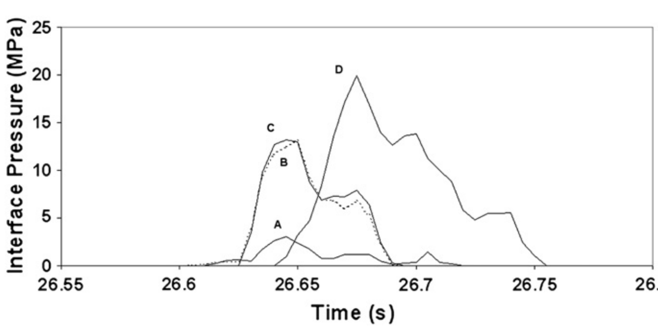

Fig. 7. Interface pressure versus time for four grillage plating elements A, B, C and D. Fig. 8 shows the locations of the elements relative to two frames and a stringer.

even more. Consequently simulations like the present one can be run in much shorter time periods.

The 'switched on' incarnation of the ice knob has realistic properties. Its brick elements have the properties of a crushable foam, as defined by Gagnon and Derradji-Aouat (2006). This material model has been validated in simulations of impacts on actual growlers in lab tests (Gagnon, 2004b; 2007) and simulations of the CCGS Icebreaker Terry Fox impacts with a bergy bit in the field (Gagnon and Derradji-Aouat, 2006; Gagnon et al., 2008). The ice knob has no contact definition with the water or the large size shell elements of the vessel. It does, however, have a contact definition with the small mesh elements of the grillage segment, as required. The fact that the ice knob has no interaction with the water is not of any significance because it is a relatively tiny part of the whole ice mass.

Since the collision of the vessel and ice mass will involve sliding to a significant extent a crushing friction coefficient was included in the contact definition for the ice knob-grillage contact. The crushing friction data from Gagnon and Mølgaard (1989) were used for this purpose. However, extrapolating that data to the sliding speed of the simulation yields a very low friction coefficient and friction can therefore be considered as negligible in the simulation results. Though it was not relevant in the present simulation we mention this because for slow speed collisions ice-structure friction could be a factor.

Following the small deck restart the ice knob and grillage can interact and the simulation runs to the point where contact occurs and the two objects behave as their properties dictate. Fig. 5 shows simulation image pairs of grillage damage (left) and interface pressure distribution (right) during the bergy bit impact. The respective image pair times from top to bottom are 26.675 s, 26.825 s, 26.975 s, 27.125 s and 27.275 s. The grillage load record for the event is shown in Fig. 6. The right hand images in Fig. 5 have had the frame and stringer components partially removed to make the pressure patterns more visible. The fourth image pair occurred just after rupture started. The ice knob, located on the outside face of the grillage, is white in the left hand images and blue in the right hand images. Slight indenting of the grillage plating and bending of frames and stringers is evident in the first image pair. More bending, accompanied by progressively more pronounced buckling of the frames, is evident in subsequent image pairs (left). Eventually rupture starts by the fourth image pair and is quite evident in the final image pair where a linear rupture can be seen in the direction of sliding along with another rupture near its trailing end that is perpendicular to it. Some stringer and frame elements also fail in the latter stages of the event, such as at the frame at the bottom of the vertically oriented rupture in the last left hand image. In that area the frame could not buckle easily to relieve stress, as in other areas, since it was kept upright by the adjacent stringer. This led to stress concentration and tearing of the frame itself. A related noteworthy feature in the right hand images is that higher interfacial pressures are evident at the plating areas that are backed by the frames and stringers, particularly where they intersect. To illustrate this more clearly Fig. 7 shows the time series for interface pressure on four plating elements at various locations with respect to two frames and a stringer (Fig. 8). As expected element A shows the least pressure and elements B and C show higher and roughly equal values. The highest pressure of the four elements is for element D that is situated near the intersection of a frame and a stringer. The highest pressure registering anywhere on the grillage plating during the collision simulation was 27.5 MPa that occurred at another stringer/frame intersection. Roughly speaking, the range of interface pressure seen in the simulation is not uncommon in crushing and impact experiments on polycrystalline ice (e.g. Gagnon and Bugden, 2008; Gagnon and Gammon, 1997; Gagnon et al., 2009).

The rupture of grillage plating and tearing failure of support structure behind the plating is facilitated by the LS-Dyna command '*MAT_ADD_EROSION'. Any element of the steel grillage that

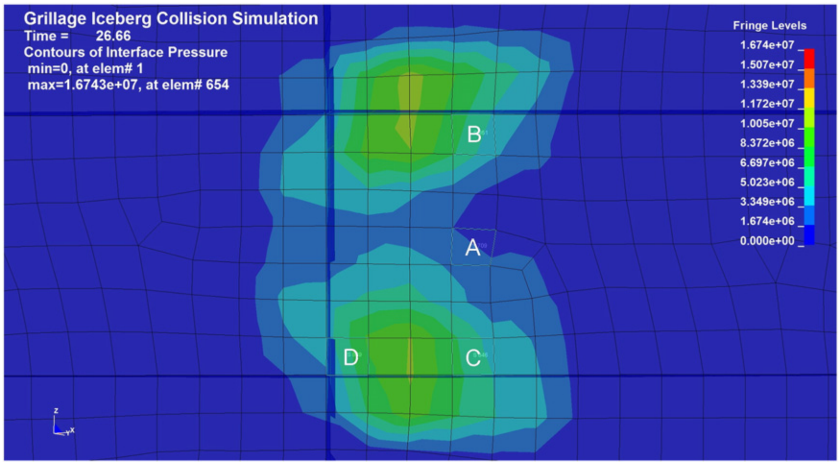

Fig. 8. Locations of the four grillage plating elements A, B, C and D, referred to in Fig. 7, with respect to two frames and a stringer.

experiences an equivalent stress of a certain value specified by the user (600 MPa in our case) will erode, that is, it disappears and no longer participates in the simulation.

The general features of damage described above, up to the point where rupture begins, are similar to results from actual grillage damage tests performed in the lab (Daley et al., 2007) and from reasonably accurate simulations of similar experiments using LS-Dyna (Quinton et al., 2010). In those experiments and simulations bending and buckling of the frames was evident in response to damaging loads. In the lab experiments pressure was not directly measured so we cannot compare with interface pressures generated in our simulation, however, load measurements were made for a case where load was applied near a constrained end of a single frame that was substantially deflected. This is a similar situation to the deflection of the frames in the last image pair of Fig. 5 where the ends of the frames are constrained because the edge of the grillage is attached to the rigid attachment frame. In our simulation the pressure map in the right image shows where the load was being applied to the fames that were undergoing substantial bending/buckling deformation (left image) and still supporting load. The images basically indicate that the second to the fifth frames from the top of the grillage and the seventh frame were deforming and supporting load. The sixth frame, located in the vicinity of the horizontal rupture had failed and did not support much load, as seen in the right image. Hence, we may calculate that the load required to highly deform a single frame in the lab test program (1.47 MN) multiplied by the number of frames that were highly deformed and supporting load in our simulation (5 frames) gives a total load of roughly 7 MN. This compares reasonably well with the load that occurred at the time of the last pair of images in Fig. 5, i.e. ~6 MN.

As previously mentioned the collision is a glancing-blow type event where the ice contact slides along the side of the vessel. This is a common scenario for collisions of ships and bergy bits. It can also occur in the case of full size icebergs, the most famous case being the Titanic incident. Our simulation shows that eventually the plating begins to rupture and rip along the grillage segment since the steel had been given a certain rupture strength (600 MPa). This kind of damage is reminiscent of documented ship-ice collision accidents such as the bulk carrier Reduta Ordona incident at the mouth of Hudson's Bay in 1996 (Fig. 9) and the sinking of the MS Explorer in the Antarctic in 2007 (MS Explorer Report, 2009).

5. Other observations and further discussion

The motion of the ice mass in response to the bow wave of the ship appears to be realistic since there is a certain degree of surge, sway and rotation of the mass before contact occurs (Figs. 10 and 11). During the 9–20 s time segment it is interesting that there is a small amount of negative sway (Fig. 10), that is, sway towards the vessel track before the vessel gets close to the ice mass. This occurred because the long axis of the ice mass was initially at an angle to the ship track. When the ice mass surged in response to the ship's bow

Fig. 9. Image showing damage to the bulk carrier Reduta Ordona resulting from a sliding-type ice collision below the waterline. The prominent gouging-type rupture is similar to that which occurred in the present simulation. (Photo credit: Andrew Kendrick).

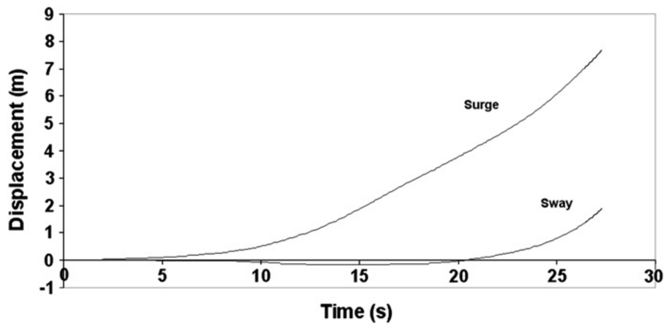

Fig. 10. Ice mass surge and sway time series. Surge and sway were determined from the motion of the center of mass of the bergy bit in response to the ship's bow wave.

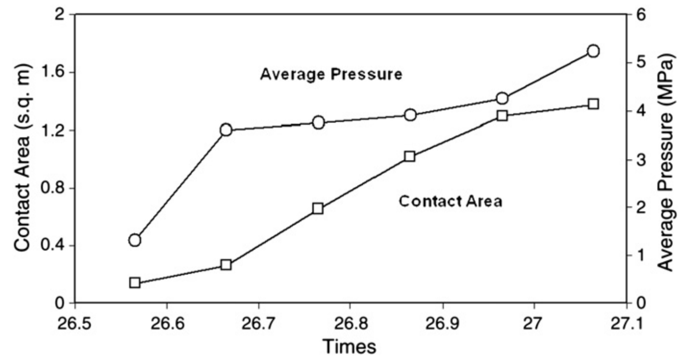

Fig. 12. Ice contact area and average pressure time series.

wave pushing the mass' leading face its angular orientation in the water caused the mass to tack sideways in the negative sway direction by a small amount before the ship was close enough to cause positive sway.

One issue that could be raised regarding the simulation results is the question of the effect of the size of the deformable grillage segment. Recognizing that the greatest damage would be in the vicinity of the contact zone one could nevertheless argue that in the real case some damage could have occurred well outside of the local region where the ice contacted the grillage segment, indeed even beyond the boundary of the grillage segment. This question could be addressed by varying the size of the grillage segment. Here, however, we are primarily concerned with describing the methods and techniques used to enable this type of simulation. Varying the size of the grillage segment, along with other parameters such as vessel speed, vessel size, ice mass size and shape, remain as tasks for future study.

For the convenience of using a half-ship in this particular simulation, that enabled us to use fewer ship and water mesh elements, we have constrained the ship to prevent yaw and roll. This is a reasonable approximation because we are assuming the vessel is a massive loaded tanker. The ship would also have a huge added mass associated with any lateral movement in the water. A rough calculation of yaw, using the moment of inertia of the vessel about a vertical axis and an average load (from Fig. 6) applied at the forward bow for the impact duration that we simulated yields a tiny fraction of a degree of rotation of the vessel about the vertical axis that would have little influence on the results presented here. Furthermore, since the load is applied to a vertically oriented grillage segment at the same approximate vertical elevation as the center of mass of the vessel there is no roll associated with the impact. In any case, the moment of inertia in the roll direction is also very substantial. Of course, it is a simple matter of altering the restraints in the LS-Dyna k-file so that movement of smaller and/or lighter vessels, in response to the collision forces, would be enabled. The same can be done in the case of a massive ship in a very low speed collision scenario where the response of the vessel could be substantial. We remind the reader that the purpose of this paper is to show the techniques that were utilized to deal with the various challenging aspects of simulations such as this and to show that reasonable results were obtained. The simulation we chose to conduct, while having a few justifiable simplifications, corresponded to a realistic scenario and was adequate for these purposes.

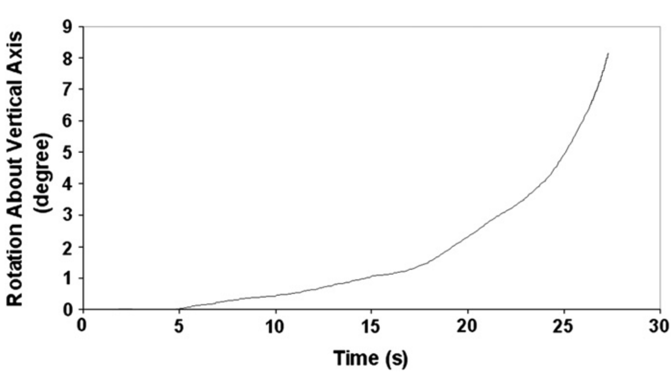

Fig. 11. Ice mass rotation time series. The rotation is about the vertical axis passing through the center of mass of the bergy bit.

Some of the analysis involved determining the relationship between average pressure over the ice contact area as the contact area varied. Figs. 6 and 12 show the load, contact area and average pressure time series for the simulation. The average pressure over the ice contact region was obtained by first determining what the contact area was. This was accomplished by viewing the grillage at specific instants in time where at each instant the interface pressure was shown for the grillage elements (e.g. Fig. 5). By choosing an appropriate scale for the colored pressure display, in our case using the range 0.001–2 MPa, the contact area could be obtained by summing the individual areas of all elements showing any indication of interface pressure. The average pressure was determined for the set of elements that were in contact with ice at that particular instant in time (e.g. Fig. 13) by dividing the total force on the grillage by the contact area. Hence, a plot of pressure versus area could be generated for the collision. Fig. 14 shows pressure versus area at six instants in time corresponding to the data points presented in Fig. 12. Roughly speaking, the pressure increases as the contact area increases. This is at odds with the well-known and frequently debated decreasing trend of nominal pressure with increasing nominal contact area reported by Sanderson (1988). However, an increasing trend of pressure with area was also observed on hard zones during the bergy bit collisions with the CCGS Icebreaker Terry Fox (Gagnon, 2008).

Looking at the pressure-area data in Fig. 14 in more detail we note that initially (between the first two data points at the left) there was a marked increase in pressure with area. Yield had started at around time 26.62 s, i.e. between the first two points. Then pressure appeared to reach a plateau as yield continued in the grillage apparently until the ice contact was passing under the second stringer (third image pair in Fig. 5) causing a rise again in average pressure. Rupture started shortly after the last data point in Fig. 14.

A similar study to the present one, involving simulations of a ship collision with a bergy bit, has been conducted by Liu et al., 2011. It is difficult to compare our results with those results because the scenarios in both studies are very different. The grillage in the other study had a different configuration and was much stronger than the present case. Furthermore, that work did not incorporate water (i.e. hydrodynamics) so the ice mass was not a free floating object and its velocity against the vessel was fixed. Also the collision was not a sliding load scenario. Perhaps the most important difference was the ice model used that had

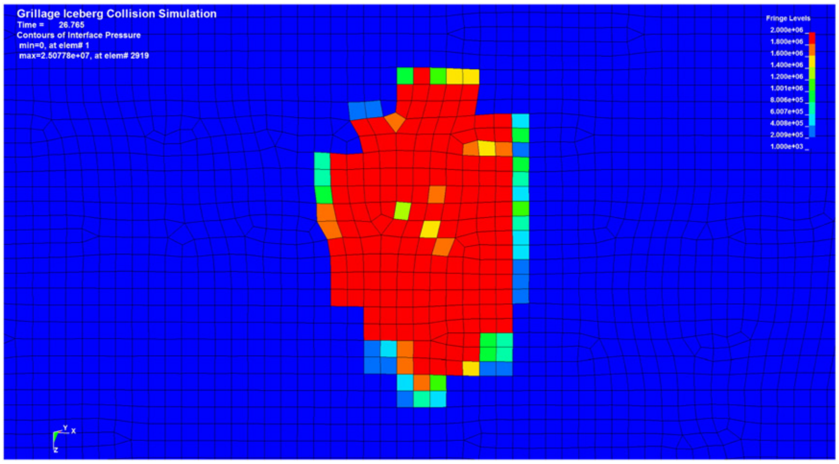

Fig. 13. Sample image illustrating how the ice contact area (Fig. 12) was determined. The summation of the individual areas of all elements showing any indication of interface pressure gives the contact area.

mesh elements that eroded in response to a critical stress. That led to the formation of gaps in places in the ice contact zone where elements disappeared. That may explain why the simulation did not appear to reflect the structure of the grillage in the pressure distribution patterns it produced. On the other hand, the damage to the grillage had some similarities with the present results such as the apparent bending and buckling of structural members behind the plating.

Finally we note that the ice model we used for the ice knob yielded reasonable results. Of course no in situ actual load or pressure distribution measurements have ever been made in the case of a structure undergoing damage due to ice crushing. However, we can get a rough idea of the ice model's capability by comparing the load that it generated at a time before rupture occurred with results from a test from the Hobson's Choice Ice Island experiments where a pyramid-shaped ice feature (test TFR#3) had generated a load of roughly 8 MN at the point in the test where it had been crushed to a depth of 78 mm. In the present simulation the load just before rupture initiated (~ 7 MN), where the ice knob has been compressed (i.e. 'crushed') by 78 mm, was reasonably close to the field result. The square top of the truncated pyramid was 500 mm × 500 mm in size and the slope of the pyramid's sides was 18° from horizontal. From a geometrical perspective the shape and dimensions of the ice knob and the truncated pyramid would generate similar degrees of confinement for crushing penetrations in the range of 78 mm. Hence, the comparison of loads is a valid exercise.

6. Conclusions

The first simulations of a collision between a bergy bit and a loaded tanker that includes hydrodynamics, a validated ice model and damage to the vessel have been performed. The results show realistic grillage damage characteristics similar to actual grillage damage tests performed in the lab. The eventual rupture of the grillage was reminiscent of gouging-type ruptures that have been observed in documented accidents. The ice model appeared to perform well, producing pressure distributions of rich texture that reflected the actual structural members (frames and stringers) of the grillage. An analysis of contact area and average pressure over the area showed that pressure increased with area. Movements of the ice mass associated with the bow wave of the vessel appeared to be reasonable. The numerical techniques employed for this simulation should make simulations of a wide variety of ice interaction scenarios with vessels and structures feasible.

An extensive program of simulations is planned for the future. The influences of ship speed and impact trajectory, and ice mass size, shape and orientation will be studied for a variety of vessel and grillage types. In the simulation above the vessel was very massive so it was valid to assume the ship motions in response to the collision, for the brief period of contact that was simulated, could be ignored. In future simulations, where appropriate, the ship motions arising from impacts will be included.

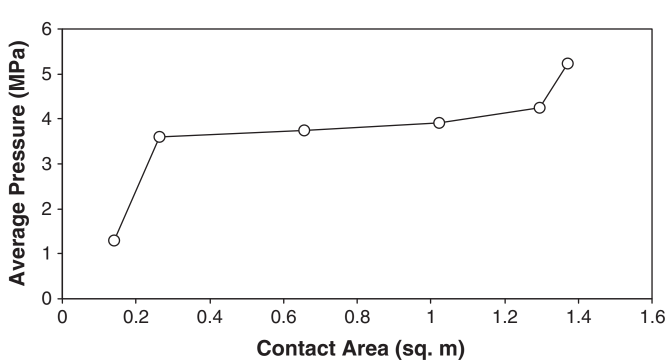

Fig. 14. Average pressure versus ice contact area for the bergy bit–ship collision up to the point just before rupture occurred. The plot shows pressure versus area at six instants in time corresponding to the data points presented in Fig. 12.

Acknowledgements

The authors would like to thank the Program of Energy Research and Development (PERD), Transport Canada and NRC for their support of this research.

References

Daley, C., Hermanski, G., Pavic, M., Hussein, A., 2007. Ultimate strength of frames and grillages subject to lateral loads—an experimental study. 10th International Symposium on practical design of ships and other floating structures. Houston, Texas.

Gagnon, R., 2004a. Physical model experiments to assess the hydrodynamic interaction between floating glacial ice masses and a transiting tanker. Journal of Offshore Mechanics and Arctic Engineering 126 (4), 297–309.

Gagnon, R., 2004b. Analysis of laboratory growler impact tests. Cold Regions Science and Technology 39, 1–17.

Gagnon, R., 2004c. Side-viewing high-speed video observations of ice crushing. Proceedings of IAHR 2004, St. Petersburg, Russia, vol. 2, pp. 289–298.

Gagnon, R., 2007. Results of numerical simulations of growler impact tests. Cold Regions Science and Technology 49, 206–214.

Gagnon, R.E., 2008. Analysis of data from bergy bit impacts using a novel hull-mounted impact panel. Cold Regions Science and Technology 52, 50–66.

Gagnon, R., 2011. A numerical model of ice crushing using a foam analogue. Cold Regions Science and Technology. 65 (3), 335–350.

Gagnon, R.E., Bugden, A., 2008. 2-Dimensional edge crushing tests on thick sections of ice confined at the section faces. Proceedings of IAHR 2008, Vancouver, Canada, vol. 2, pp. 973–981.

Gagnon, R.E., Derradji-Aouat, A., 2006. First Results of Numerical Simulations of Bergy Bit Collisions with the CCGS Terry Fox Icebreaker. Proceedings of IAHR 2006, Sapporo, Japan.
Gagnon, R.E., Gammon, P.H., 1997. In-situ thermal profiles and laboratory impact experiments on iceberg ice (1997) Journal of Glaciology 43 (145), 569–582.
Gagnon, R.E., Mølgaard, J., 1989. Crushing friction experiments on freshwater ice. Proceedings of the IUTAM/IAHR Symposium on Ice/Structure Interaction, Aug. 1989, Newfoundland, Canada, pp. 405–421.
Gagnon, R., Cumming, D., Ritch, A., Browne, R., Johnston, M., Frederking, R., McKenna, R., Ralph, F., 2008. Overview accompaniment for papers on bergy bit impact trials. Cold Regions Science and Technology 52, 1–6.
Gagnon, R.E., Bugden, A., Ritch, R., 2009. Preliminary testing of a new ice impact panel. Proceedings of POAC 2009, Lulea, Sweden. Paper No. 33.
Hallquist, J.O., 1998. LS-Dyna Theoretical Manual. Livermore Software Technology Corporation. May 1998.
Jones, S.J., Gagnon, R.E., Derradji-Aouat, A., Bugden, A., 2003. Compressive strength of iceberg ice. Canadian Journal of Physics 81 (1 / 2), 191–200.
Liu, Z., Amdahl, J., Løset, S., 2011. Integrated numerical analysis of an iceberg collision with a foreship structure. Marine Structures 24 (4), 377–395.
MS Explorer Report, 2009. Decision of the Commissioner of Maritime Affairs, R.L. and the Report of Investigation in the Matter of Sinking of Passenger Vessel EXPLORER (O.N. 8495), 23 November 2007 in the Bransfield Strait near the South Shetland Islands. Published by the Bureau of Maritime Affairs, Monrovia, Liberia. 26 March, 2009.
Quinton, B., Daley, C.G., Gagnon, R.E., 2010. Effect of moving ice loads on the plastic capacity of a ship's structure. Icetech 2010. Anchorage, Alaska.
Sanderson, T.J.O., 1988. Ice Mechanics: Risks to Offshore Structures. Graham and Trotman, London.